Title	White-light-induced annihilation of percolation paths in SIO2 and high-k dielectrics - prospect for gate oxide reliability rejuvenation and optical-enabled functions in CMOS integrated circuits
Author(s)	Ang, Diing Shenp; Kawashima, Tomohito; Zhou, Yu; Yew, Kwang Sing; Bera, Milan Kumar; Zhang, Haizhong
Citation	Ang, D. S., Kawashima, T., Zhou, Y., Yew, K. S., Bera, M. K., & Zhang, H. (2015). White-light-induced annihilation of percolation paths in SIO2 and high-k dielectrics - prospect for gate oxide reliability rejuvenation and optical-enabled functions in CMOS integrated circuits. ECS Transactions, 69(5), 169-181.
Date	2015
URL	http://hdl.handle.net/10220/45197
Rights	© 2015 The Electrochemical Society. This is the author created version of a work that has been peer reviewed and accepted for publication by ECS Transactions, The Electrochemical Society. It incorporates referee's comments but changes resulting from the publishing process, such as copyediting, structural formatting, may not be reflected in this document. The published version is available at: [http://dx.doi.org/10.1149/06905.0169ecst].

White-Light-Induced Annihilation of Percolation Paths in SiO_2 and High-k Dielectrics – Prospect for Gate Oxide Reliability Rejuvenation and Optical-Enabled Functions in CMOS Integrated Circuits

D. S. Ang[a], T. Kawashima[a,b], Y. Zhou[a], K. S. Yew[a], M. K. Bera[a], and H. Z. Zhang[a]

[a] Nanyang Technological University, School of Electrical and Electronic Engineering, Nanyang Avenue, Singapore 639798, Singapore
[b] Toshiba Corporation, 33, Shin-Isogo-Cho, Isogo-ku, Yokohama 235-0017, Japan

The formation of nanoscale percolation paths or conducting filaments in oxide materials such as SiO_2, HfO_2, etc. presents both a challenge to gate oxide reliability as well as an opportunity to a next-generation resistive memory technology, as these materials have already been heavily deployed in mainstream integrated circuit manufacturing. In this paper, we present novel experimental evidence showing that electrical conduction through a nanoscale conducting filament can be disrupted upon illumination by white light. The disruption is either permanent or temporary, depending on the current which passed through the filament at the instant of its formation before the process was interrupted. The underlying mechanism is believed to involve photon-induced migration of neighboring interstitial oxygen ions, leading to their recombination with the vacancy sites which made up the conducting filament. This finding suggests possible exploitation for gate oxide reliability renewal and implementation of optical functions in SiO_2 or HfO_2 based devices whose functionality thus far is only limited to electrical excitation.

Introduction

Gate oxide breakdown, an outcome whereby the dielectric loses its insulating property, has been a well-known front-end reliability challenge for advanced complementary metal-oxide-semiconductor (CMOS) technology that features SiO_2 with thickness less than ~5 nm (1). In recent CMOS technology nodes, the traditional polysilicon/SiO_2 gate stack has been replaced with a metal/high-k gate stack in order to fulfill the gate leakage-current and equivalent capacitance scaling requirements. With this change, gate oxide breakdown is expected to become an even more pressing issue owing to the generally low breakdown electric field of high-k dielectrics (2) and the inevitable presence of a low quality Si sub-oxide layer at the interface between the high-k dielectric and the channel (3). Although the exact mechanism of gate oxide breakdown is yet to be confirmed, the process is broadly believed to involve the random generation of oxide defects under electric field and temperature stressing. The local increase in gate current and the associated thermal heating, as a result of the clustering of oxide defects, would then set off a positive feedback cycle that eventually leads to a short-circuit between the gate and channel (4). Leveraging on advanced atomic-scale characterization techniques, the location of the breakdown site, commonly termed as the percolation path, was shown to

be oxygen deficient (5). Thus, electrical-cum-thermal induced generation of oxygen-vacancy defects has been commonly identified as the intrinsic cause of gate oxide breakdown.

Studies have found that breakdown involving relatively thin gate oxides (of ~5 nm or less in thickness) may not always lead to a total loss of transistor functionality, unlike in cases involving thick oxides (6). The breakdown mode of thin gate oxides has been termed soft breakdown so as to distinguish it from the catastrophic hard breakdown (HBD) associated with thick oxides. While the exact reasons for SBD are yet to be completely established, it is believed to have been caused by the typically lower gate stress voltage used. As a consequence, the surge in current during breakdown transient is decreased or could be aborted in time to avoid the thermally induced structural changes that typically characterize HBD. The non-destructive nature of SBD has generated considerable interest in understanding the mechanisms that govern post-SBD evolution towards HBD, which would aid in assessing the additional reliability margin offered by SBD (7). Apart from the retention of transistor functionality, another notable difference between SBD and HBD lies in the ability of the former to exhibit a partial or complete recovery effect, which occurs either upon stress termination (8), during post-breakdown electrical measurement (9), or after thermal annealing (10), (11). The extent of recovery is found to depend greatly on the types of dielectric and gate stack structure, as well as the level of current through the percolation path before the breakdown is interrupted (i.e. breakdown hardness). For instance, electrically induced breakdown recovery is found to occur more readily in the metal/high-k gate stack as compared to the polysilicon/SiO_2 gate stack (9), (12). Breakdown recovery in the latter can generally be achieved only by thermal annealing (10), (11). Studies which observed a dependence of breakdown recovery on metal gates with varying oxygen solubility (12) lend strong support to the proposed oxygen-vacancy defect model.

Although gate oxide breakdown presents a critical reliability issue threatening the useful lifespan of CMOS integrated circuits, recent years have seen it being exploited for next-generation resistance-switching random access memory (RAM), most notably in valence-change type of resistive memory or ReRAM devices involving transition metal oxides such as HfO_2, Ta_2O_5, etc. (13), (14). Operation of this class of resistive memory devices first requires subjecting the oxide layer to a high voltage/oxide field to create a nanoscale conducting filament (akin to the ramped-voltage or constant voltage stressing that leads to the generation of an oxide percolation path), which places the device in a low resistance state. Subsequent repetitive switching between the low and a high resistance state is believed to occur via dissolution (partial or complete) and reformation, respectively, of the conducting filament through oxygen interchange with the metal electrodes, enabled by a series of alternating voltage polarities applied to the electrode (15). While the resistance-switching operation is typically accomplished by electrical stimulation, some studies have demonstrated light-enabled multi-level resistance switching in narrow bandgap oxides (e.g. ZnO) and perovskites (16)-(19).

In this paper, we summarize our recent experimental evidence showing that electrical conduction through a nanoscale conducting filament in the SiO_2, HfO_2 and ZrO_2 dielectrics can be disrupted upon exposure to white light (20), (21). To-date, optical stimulation of these dielectrics for realizing device functionalities has seldom being explored, owing to the lack of photosensitivity in these materials. Because of their large

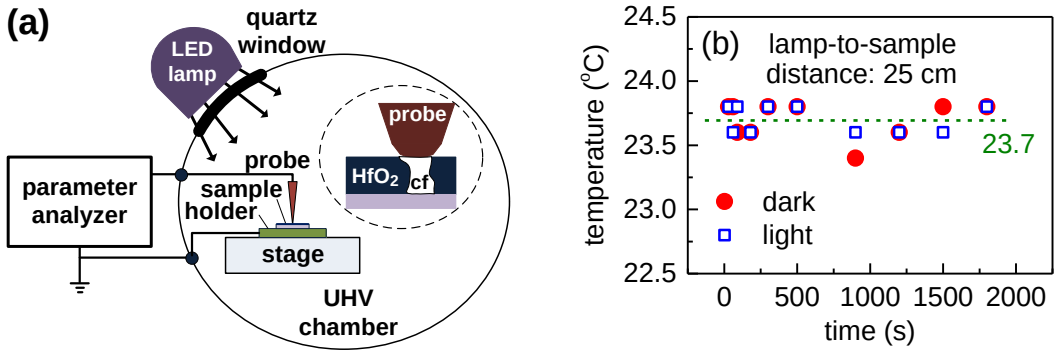

Figure 1. (a) Schematic illustration of the experimental set-up. The inset is a magnified view of the probe-to-sample contact region, showing the probe contacting a nanoscale conducting filament (cf) formed in HfO_2. (b) Sample temperature (measured by an infrared thermometer) as a function of time in the dark and under white-light illumination. Dashed line depicts the average temperature for both cases.

bandgaps (> 5 eV), studies were only limited to the deep ultra-violet regime and beyond, addressing post-irradiation reliability issues (22), (23). In our study, it was found out that after these oxides had suffered SBD, the breakdown site became photo-responsive, in that its electrical conductivity can be decreased upon white-light illumination. The extent of decrease depends on the light intensity and exposure time, enabling intermediate resistance values to be achieved through adjustments of these parameters. We termed the observed behavior "negative photoconductivity", as a contrast against the photoconductive response of narrow bandgap oxides and perovskites. The photosensitivity of SBD SiO_2, HfO_2 and ZrO_2 points towards the possible incorporation of optical functionality into mainstream CMOS integrated circuits.

Experimental Details

In view that the top electrode in the polysilicon/SiO_2/Si, metal/high-k/Si and metal/high-k/metal stacks generally has very low optical transmittance (due to significant surface absorption/reflection), our study was carried out on uncapped samples, consisting of SiO_2/p-Si, HfO_2/p-Si, HfO_2/TiN/Ti/p-Si, ZrO_2/TiN/Ti/p-Si and SiO_2/Cu/Ti/p-Si stacks in an ultra-high vacuum (UHV) conductive atomic force microscope (C-AFM) system (RHK 3500 HT AFM/STM). The C-AFM probe was made up of diamond-coated Si, which performed the role of a top electrode mimicking a metal-oxide-Si (MOS gate stack) or metal/insulator/metal (ReRAM) structure of a very small dimension. From the force-distance relationship and the mechanical properties of the cantilever (24), the probe-to-oxide contact area was estimated to be 26 nm^2. The UHV environment helped avoid surface contamination. The SiO_2 was 5-nm thick for the SiO_2/p-Si sample and 10-nm thick for the SiO_2/Cu/Ti/p-Si sample, formed by a conventional plasma-enhanced chemical vapor deposition process. The HfO_2 and ZrO_2 were each of thickness 4 nm and were grown by an atomic-layer deposition process. Before the oxide deposition step, sputter-deposition of a 10-nm or 30-nm Ti layer, followed by a 70-nm TiN or 30-nm Cu layer, respectively, on a pre-cleaned p-Si substrate were carried out to form the bottom metal electrode in some of the test samples. For simplicity, only the type of oxide and the metal electrode in contact with the oxide will be referenced in subsequent discussion.

Fig. 1(a) is a schematic illustration of the experimental set-up. Voltage biasing of a test sample was applied through the C-AFM probe, connected to a Keithley SCS4200 parameter analyzer. The Si substrate was always grounded. Formation of the conducting filament was achieved in two ways: 1) a voltage-ramp; 2) a constant-voltage applied to the C-AFM probe. In both cases, the current through the filament at the instant of its formation was capped at a preset level, termed the current compliance, by the parameter analyzer. White light, with a wavelength range of 450-700 nm, was supplied by an ordinary LED lamp positioned at the quartz window of the UHV chamber, at about 25 cm away from the test sample. The intensity of light reaching the sample surface was estimated using a Daystar's DS-05A solar meter placed 25 cm away from the LED lamp. All results are obtained at an intensity of 1 mW/cm^2 unless stated otherwise. Possible sample heating by the white-light illumination was checked using an infra-red thermometer. Fig. 1(b) shows the sample temperature recorded at selected intervals over a period of 30 minutes in the dark and in the presence of white-light illumination. Fluctuations in the measured sample temperature are less than 0.5 K, indicating that the illumination did not result in any significant heating effect even under a prolonged period.

Results and Discussion

In this section, we present consistent experimental evidence showing that white-light illumination can eliminate the increased leakage current that flows through the percolation path or conducting filament formed in an oxide by electrical stressing. Results for different oxide materials (HfO_2, ZrO_2 and SiO_2) and different bottom electrode materials (TiN, Cu, Si) will be discussed. In the context of ReRAM, the observation can be referred as light induced resistance reset. In the context of gate oxide integrity, the observation may be referred as light assisted breakdown recovery. The successful restoration of the breakdown oxide region by white light is further confirmed by subsequent electrical-stress test, where a similar "robustness" to stress induced breakdown is observed. We attribute the physical phenomenon to the elimination of oxygen-vacancy defects that form the percolation path, via recombination with photo-stimulated migrating oxygen ions.

White-Light Induced Disruption of Filamentary Conduction

Fig. 2(a) depicts the impact of white-light illumination on electrical conduction through a percolation path in the HfO_2/TiN sample. The percolation path was formed at a current compliance of 100 nA by a positive voltage-ramp applied to the C-AFM probe (line; Fig. 2(b)). After filament formation, a constant voltage of 1 V was applied to the C-AFM probe and the current through the filament monitored as a function of time in the dark. A progressive current decay is evident (circle; Fig. 2(a)), due to post-electrical-stress relaxation. The relaxation approached quasi-saturation after $\sim 2\times10^3$ s, as is evident from the relatively constant current obtained when the measurement was restarted (square). After $\sim 1\times10^3$ s, the sample was illuminated with white light, with an estimated intensity of 1 mW/cm^2 at the sample surface. During illumination, the current decreased abruptly to the measurement floor and it remained at this level after the light was turned off. Since the current was stable for a long period prior to the white-light exposure, the role of thermal induced probe drift on the current decrease may be excluded. The observation thus shows that electrical conduction through the filament was disrupted

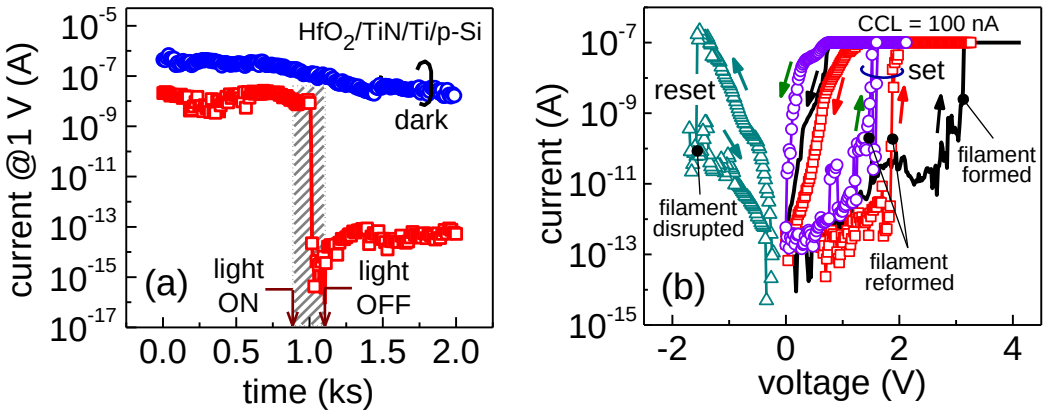

Figure 2. (a) Current versus time characteristics of a nanoscale conducting filament formed in HfO_2. Circle - first measurement carried out immediately after filament formation; square - second measurement with an intermittent white-light exposure. (b) Dual voltage-sweep measurements performed in the order stated: filament formation (black); filament reformation (i.e. set) after the light-induced disruption or reset in (a) (square); filament disruption by an opposite-polarity sweep; filament reformation after electrical induced filament disruption.

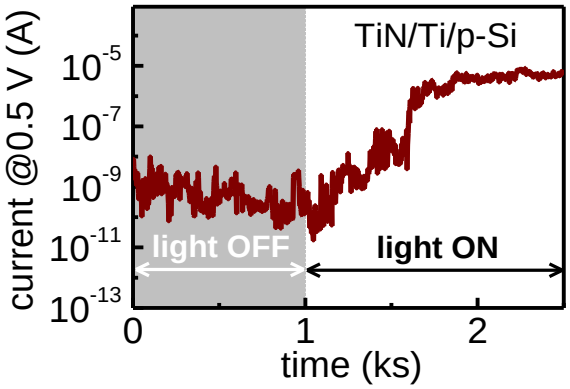

Figure 3. White-light illumination results in an increase in the current through the control sample (without an oxide layer).

upon white-light illumination, i.e. the resistance of the breakdown path was "reset" to a higher level by the light. A positive-voltage sweep measurement performed after the light induced reset (LIR) reveals a current comparable to that before the filament was first formed (square; Fig. 2(b)), confirming that the breakdown path had been "repaired". However, reformation of the filament now occurred at a lower voltage (~2 V) compared to that of the first formation (~3 V). This shows that although white light could restore the resistance of the breakdown oxide, the chemistry of the restored oxide region may differ from that present before the first breakdown. After the filament was reformed, it was subjected to a negative-voltage sweep during which a significant decrease in current was observed (triangle). This behavior is typical of the bipolar reset characteristic of the HfO_2 ReRAM device. Following this electrical induced reset, a subsequent positive-voltage sweep resulted in filament reformation at nearly the same voltage (diamond) as that after LIR. This implies that the effect of LIR is similar to that of an electrical induced reset.

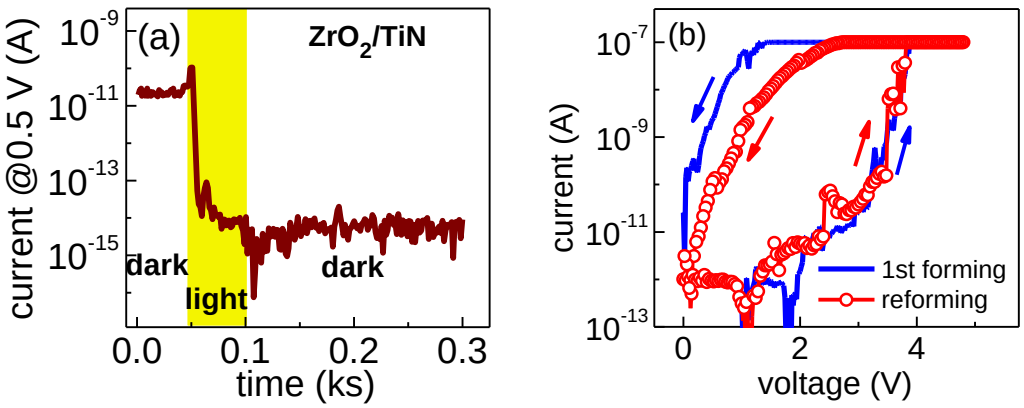

Figure 4. (a) Current-time characteristic showing disruption, upon white-light illumination, of electrical conduction through a percolation path formed in ZrO_2. (b) Current-voltage curves for the same location depicting percolation path formation and reformation after white-light illumination. Arrows denote directions of voltage sweep beginning at 0 V. Due to the different lower limits of the current measurement range (100 pA for (a) and 10 nA for (b)), the current "floors" differ correspondingly.

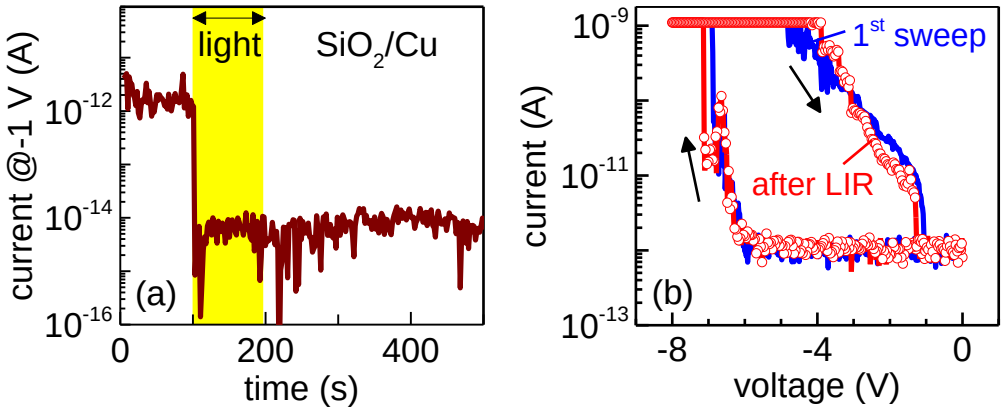

Figure 5. (a) Current-time characteristic showing light induced reset in the SiO_2/Cu/TiN stack. (b) Current-voltage curves showing the first formation of the conducting filament and reformation after light induced reset. Arrows denote directions of voltage sweep beginning at 0 V.

To further verify that the current decrease observed under illumination (Fig. 2(a)) is a result of the disruption of the conducting filament in the HfO_2, conduction through a control sample (i.e. one without the HfO_2 and consisting of only the TiN/Ti/Si stack) in the dark and in the presence of white-light illumination were compared (Fig. 3). As is apparent, the current was significantly increased after the light was turned on. This behavior is totally opposite to the decrease observed on the HfO_2/TiN sample, confirming that the latter arose from the disruption of the conducting filament in the HfO_2. The increase in current in the case of the control sample may be attributed to photon absorption at the TiN surface, which yields "hot electrons" that may easily overcome the TiN-to-probe contact barrier formed by the thin surface oxide. It should be noted that the LIR effect depicted in Fig. 2(a) was also observed using a scanning tunneling microscope probe made up of Pt/Ir (with 80 atomic percent Pt), thus eliminating any possible role of the probe on the observed effect (not shown).

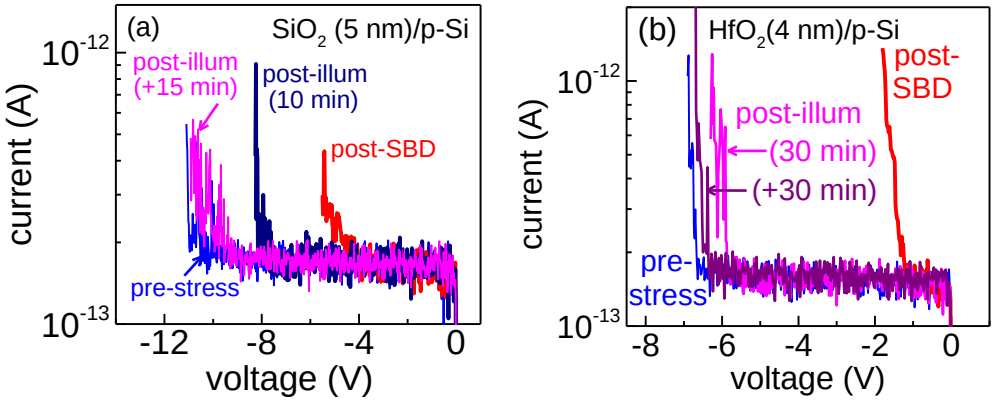

Figure 6. (a) Effect of white-light illumination on the post-SBD current-voltage characteristics of a SiO_2/Si stack. During illumination, the probe voltage was 0 V. The illumination time is given in parenthesis; '+' denotes additional illumination time. SBD was induced by constant-voltage stressing at −10 V, with a current compliance of 0.5 nA. The breakdown oxide region can be completely restored after 25 minute of illumination. (b) A similar observation applies to the HfO_2/Si stack. The sample was stressed at –6V; the current compliance was 500 nA.

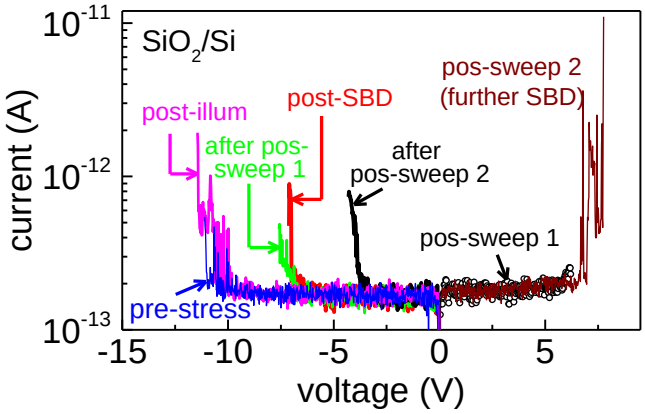

Figure 7. An opposite positive-voltage sweep is shown to have a limited effect on the recovery of the SiO_2/Si gate stack after suffering SBD during negative constant-voltage stressing. On the other hand, full recovery can be achieved via white-light illumination, even after the gate stacks had suffered further breakdown during the positive-voltage sweep.

The LIR effect can also be consistently observed on samples made up of other oxides (ZrO_2, SiO_2) as well as those having the gate stack (i.e. MOS) structure. As shown in Fig. 4(a) for the ZrO_2/TiN sample, conduction through the filament formed after SBD (via positive-voltage ramping) can be successfully disrupted when illuminated by white light, similar to that seen in the HfO_2 sample. For this location tested, filament reformation (i.e. second SBD at the same location during a post-LIR positive-voltage sweep) occurred at nearly the same voltage as that for the first SBD (Fig. 4(b)), implying that the breakdown oxide region had been restored to almost the original state. A similar LIR effect is seen in the SiO_2/Cu sample (Fig. 5) as well as in the SiO_2/Si and HfO_2/Si gate stack samples (Figs. 6(a) and 6(b), respectively). For the gate stack samples, the current-time curve was not monitored under illumination as the injection of optically generated electrons in the Si substrate also contributed to the measured current. Instead, the pre-stress, post-SBD

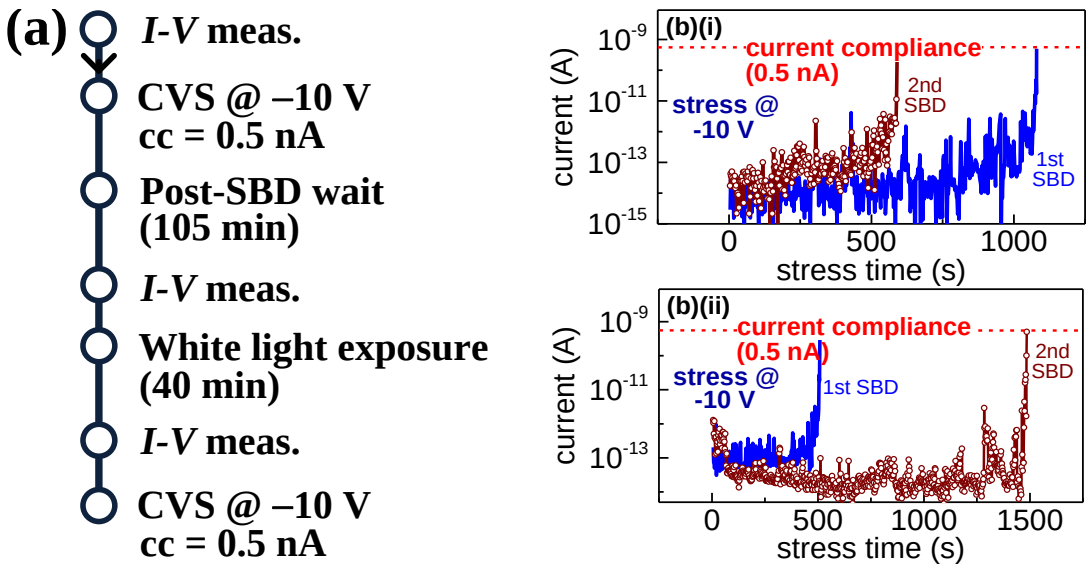

Figure 8. (a) Experimental sequence used to assess the robustness of white-light-restored oxide against electrical re-stressing under the same conditions as those used to induce the first soft breakdown. (b) A comparison of the current-time characteristics of the first and second SBD evolution, for two randomly selected locations on the SiO_2/Si sample.

and post-illumination current-voltage (*I-V*) curves are compared. The post-SBD curve was taken after post-stress relaxation effect has quasi-saturated but before white-light illumination. SBD was induced via constant-voltage stressing (CVS) and the stressing aborted by the parameter analyzer when the current surge during breakdown exceeds a preset current compliance. As is apparent for both the SiO_2/Si and HfO_2/Si stack, the post-SBD *I-V* curve is progressively shifted towards the pre-stress counterpart following white-light illumination. After a sufficiently long illumination period, the restored *I-V* curve can be seen to almost coincide with the pre-stress curve.

Since electrical induced recovery (via an opposite polarity voltage sweep) is commonly observed in the MIM ReRAM structure, it is pertinent to also examine the effect of an opposite-voltage sweep on the post-SBD recovery of gate stacks. Fig. 7 shows the results. Unlike the ReRAM structure, the gate stack structure is generally more resistant to electrical-induced recovery. As can be seen in Fig. 7 for the SiO_2/Si sample (SBD induced by negative CVS), the first positive-voltage sweep did not yield any apparent recovery of the *I-V* curve. Extending the voltage range during the second positive-voltage sweep resulted in a further breakdown, as is evident from the shift of the *I-V* curve to an even lower voltage regime. However, a nearly complete recovery was achieved by a 30-minute exposure to white-light after the second positive-voltage-sweep induced breakdown. A similar result is obtained on the HfO_2/Si sample (not shown). While this sample exhibits a more apparent recovery after a positive-voltage sweep, the extent of recovery is nonetheless limited and extending the positive-voltage sweep range leads to further breakdown, just like the SiO_2/Si sample. The results show that white-light illumination is much more efficient in inducing the recovery of breakdown gate stacks.

Electrical Robustness of White-Light Restored Oxide

A question of interest at this juncture would be the robustness of the white-light

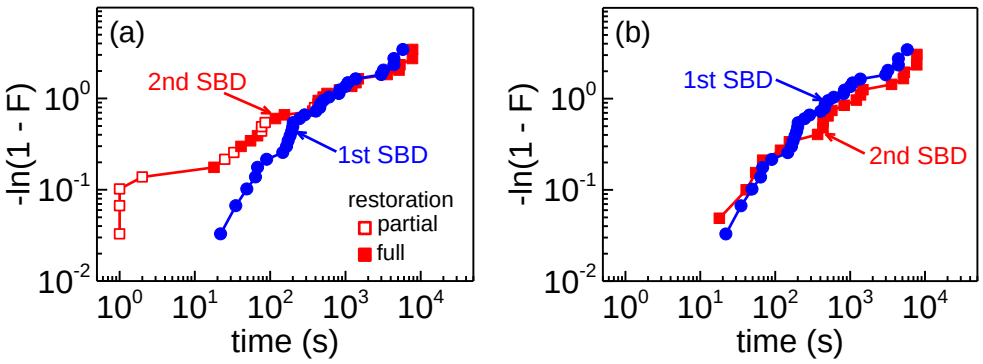

Figure 9. Weibull distributions for the time to first and second soft breakdown (SBD) for the SiO_2/Si sample. The second SBD was induced by the same negative constant-voltage stressing of the location where the first SBD occurred and had been restored by white-light illumination. A total of 30 random locations were tested. (a) second SBD data for all locations (complete and partial restored); (b) second SBD data for only those locations where full restoration had been achieved.

restored oxide against electrical re-stressing. To address this, the time-dependent dielectric breakdown (TDDB) reliability of the pristine and restored oxide are compared for the SiO_2/Si sample. The experimental sequence is summarized in Fig. 8(a). Prior to the first CVS, the *I-V* curve was measured (cf. Fig. 6). A negative CVS was then applied. Fig. 8(b) shows the evolution of the current towards the first SBD (line) for two random locations on the SiO_2/Si sample. Prior to SBD, a gradual increase of current with time can be observed, indicating the onset of a progressive breakdown behavior typical of a thin gate oxide (25). When the increase in current reached a preset compliance level, the stress was automatically aborted by the parameter analyzer. *I-V* measurement was then taken continuously in the dark to monitor the post-stress relaxation effect until quasi-saturation was reached (after ~105 minutes). The final post-SBD *I-V* curve was recorded before the sample was subjected to white-light illumination. After 40-minute illumination, the light source was removed and the *I-V* curve for the restored oxide was measured. Regardless of whether full restoration was achieved, the negative CVS was reapplied until the second SBD occurred. The same experimental procedure was repeated on 30 randomly selected locations on the SiO_2/Si sample.

For the two random locations depicted in Fig. 8(b), full restoration of the breakdown oxide was achieved as judged by overlapping pre-stress and restored *I-V* curves (cf. Fig. 6(a)). However, the time to second SBD can either be shorter or longer than the first. As the defect generation process leading to oxide breakdown is stochastic in nature, the Weibull distribution for the time to first and second SBD would have to be compared, as depicted in Fig. 9(a). In the distribution curve for the second SBD, the data points are classified according to whether full (solid) or partial (open) restoration was achieved during white-light illumination. Compared to the distribution curve of the first SBD, the distribution curve of the second SBD features a prominent “tail”, but populated mainly by the early failures, upon restressing, of locations where the breakdown oxide was partially restored by the white-light illumination, i.e. the *I-V* curves for these locations fall at a lower voltage regime than their pre-stress counterparts. At these locations, the oxide was “weaker” in comparison to the original states and thus it failed at a much shorter times when subjected to the same negative CVS. On the other hand, for locations where the breakdown oxide was fully restored, the distribution curve of the second SBD can be

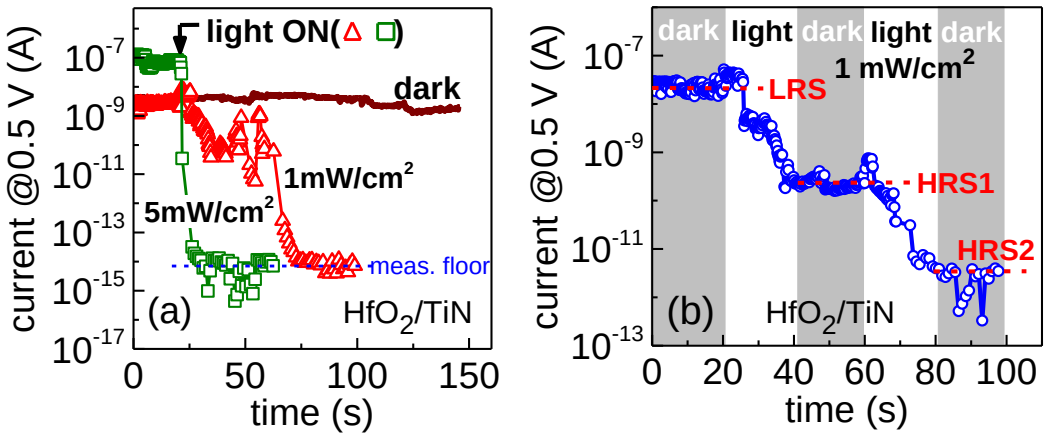

Figure 10. (a) Filament disruption occurs at a faster rate when illuminated under white-light of a higher intensity. The test was carried out at the same location on the HfO_2/TiN sample, with the filament reformed after the reset by light of the lower intensity. (b) A relatively stable current plateau (denoting an intermediate high resistance state (HRS1) between the low resistance state LRS and a second higher resistance state HRS2) can be achieved by removing the white-light illumination after 20 s. HRS2 is obtained by resuming the illumination for another 20 s.

seen to merge with that of the first SBD. This result shows that the fully restored oxide exhibits similar robustness against breakdown during electrical re-stressing. This can be verified by excluding locations where only partial restoration was achieved when plotting the Weibull distribution plot for the time to second SBD. The resultant distribution is nearly identical to that of the first SBD (Fig. 9(b)).

Effect of Light Intensity and Exposure Period

Up to this point, all results on white-light induced resistance reset or breakdown recovery are obtained with a light intensity of 1 mW/cm^2. It is of interest to also examine the impact of light intensity on the resistance reset. Results are shown in Fig. 10. Initially, white light of a lower intensity was applied to induce resistance reset after forming (triangle). Then, the conducting filament was reformed by ramping up a positive voltage followed by the exposure to white light of a five times higher intensity. As can be seen in Fig. 10(a), the current decreases more gradually under the lower intensity light exposure, as compared to the higher intensity case where the current decreases more abruptly (showing a resistance reset that occurred at a distinctively faster rate). In the case of the low-intensity light, it takes 52 s for the current to decrease to the measurement floor. As for the case of the high-intensity light, the time is 9.3 s. This 5.7-time reduction corresponds well to the difference between the two light intensities. Clearly, light intensity strongly influences the speed at which the conducting filament is disrupted. The current evolution in the absence of illumination is also shown for comparison.

As the data in Fig. 10(a) show, the change in resistance in a specific time interval is determined by the amount of light energy that the filament received, indicating a possibility of achieving multiple resistance levels for a given filament. This is indeed observed in Fig. 10(b), where different levels of the conducting filament disruption can be controlled by changing the duration of light exposure. Upon illumination, the current is decreased from the low-resistance state (LRS) to a first high-resistance state (HRS1) in

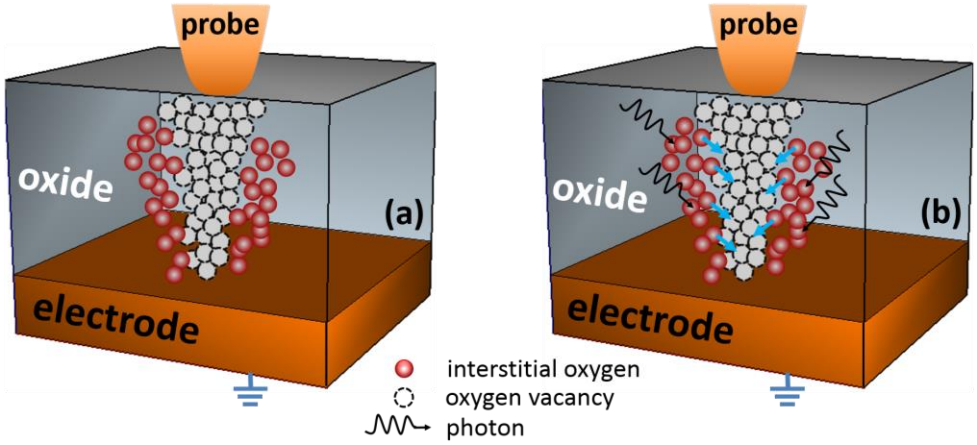

Figure 11. Physical explanation for white-light induced disruption of filament conduction: (a) Schematic diagram of the probe/oxide/electrode structure showing a conducting filament made up of oxygen vacancies. The dislodged oxygen ions occupy interstitial positions around the vacancy-filled filament. (b) Photons from the white-light source excite the interstitial oxygen ions, causing them to migrate and recombine with the vacancies in the filament.

a 20-s interval. The current decrease is obviously arrested when the light illumination is removed, as is evident from the current plateau. When the illumination was resumed, the current is decreased to the next higher resistance state (HRS2). Clearly, by controlling the light exposure, one can generate multiple resistance values for the conducting filament. This result suggests the possibility of a light-enabled ReRAM-resistance tuning approach, as an alternative to the electrical counterpart, for neuromorphic computing applications (26). The electrical tuning method might be challenging because it requires the control of a set current compliance limit (for DC switching) or set/reset pulse timing (for AC switching) (27).

Proposed Explanation

A possible explanation for the light-induced resistance reset phenomenon is illustrated in Fig. 11. Our proposed model can be supported by: 1) studies based on atomic-scale electron-energy loss spectroscopy which show that the breakdown oxide region is depleted of oxygen (5), (28), (29), i.e. the percolation path or conducting filament comprises of oxygen-vacancy defects; 2) a recent physics based simulation study showing some of the dislodged oxygen ions populating interstitial sites around the vacancy-filled conducting filament when the breakdown process is abruptly terminated (30). Fig. 11(a) depicts the formation of an oxygen-deficient conducting filament through the oxide layer when a voltage sweep is applied via the C-AFM probe. Electron transport through the oxide film induces breakage of the metal-oxygen bonds and out-diffusion (assisted by the temperature and electrical field distributions) of the released negatively charged oxygen ions, resulting in the formation of an oxygen-deficient (metal-rich) conducting filament. As the forming process is interrupted when the current reaches a compliance limit, some of the released oxygen ions remain in the interstitial positions in the vicinity of the filament and may be subsequently driven back to the filament by the applied electrical field and temperature gradient during the electrically-controlled reset (16). The diffusion of interstitial oxygen ions entails the overcoming of an energy barrier of 0.3-0.6 eV (31). At a low voltage (below the electrical reset voltage), the diffusion rate

would thus be negligibly small. It is suggested that a white light illumination generates a photon-induced excitation of the oxygen ions over the diffusion energy barrier (32), hence accelerating their diffusion towards the vacancy-rich filament, as illustrated in Fig. 11(b)**.** The ion excitation proceeds more efficiently under a stronger light intensity, thus enhancing the migration of oxygen ions back to the vacancy sites, as manifested by the faster resistance reset rate in Fig. 10(a).

Summary

Non-photo-responsive large bandgap oxide materials such as HfO_2, ZrO_2 and SiO_2 are consistently found to become photo-responsive after suffering an electrical-stress induced SBD. Unlike the classical photo-response behavior of narrow bandgap oxides and perovskites which is commonly manifested as an increase in electrical conduction due to the generation of excess charge carriers by the incident photons, the photo-response here comes in the form of a disruption of electrical conduction through the nanoscale conducting filament or percolation path formed during breakdown. When that occurs, the insulating properties of the breakdown oxide region can be restored to almost the pristine condition, as is confirmed by the similar robustness of the restored oxide against electrical-stress induced breakdown. The disruption in electrical conduction caused by white-light illumination is proposed to occur through photon-stimulated migration of interstitial oxygen ions nearby the vacancy-filled filament, resulting in the migrating oxygen ions recombining with the vacancies in the filament. This unique photo-responsive behavior, which we termed as negative photoconductivity of SBD HfO_2, ZrO_2 and SiO_2 points towards the possibility of gate oxide reliability rejuvenation as well as the incorporation of optical functions into mainstream CMOS-based integrated circuits.

Acknowledgments

Partial support from a Singapore Ministry of Education research grant MOE2013-T2-2-099 is gratefully acknowledged. Y. Zhou and H. Z. Zhang are each supported by an NTU research scholarship. T. Kawashima is supported by a Toshiba study grant.

References

1. J. S. Suehle, *IEEE Trans. Electron Devices*, **49**, 958 (2002).
2. J. W. MacPherson, J. Kim, A. Shanware, H. Mogul, and J. Rodriguez, *IEEE Trans. Electron Devices*, **50**, 1771 (2003).
3. T. Kauerauf, R. Degraeve, E. Cartier, B. Govoreanu, P Blomme, B. Kaczer, L. Pantisano, A. Kerber, and G. Groeseneken, in *Tech. Dig. Int. Electron Devices Meet.* 2002, 521.
4. J. H. Stathis, *J. Appl. Phys.*, **86**, 5757 (1999).
5. X. Li, C. H. Tung, and K. L. Pey, *Appl. Phys. Lett.*, **93**, 072903 (2008).
6. M. Depas, T. Nigam, and M. M. Heyns, *IEEE Trans. Electron Devices*, **43**, 1499 (1996).
7. E. Wu, J. Sune, B. Linder, J. Stathis, and W. Lai, in *Tech. Dig. Int. Electron Devices Meet.* 2003, 919.

8. T. Bearda, P. W. Mertens, M. M. Heyns, H. Wallinga, P. Woerlee, *Jap. J. Appl. Phys.*, **39**, L582 (2000).
9. A. Crespo-Yepes, J. Martin-Martinez, A. Rothschild, R. Rodriguez, M. Nafria, and X. Aymerich, *IEEE Electron Device Lett.*, **31**, 543 (2010).
10. W. Y. Loh, B. J. Cho, and M. F. Li, *Jap. J. Appl. Phys.*, **41**, 2873 (2002).
11. G. Ghidini, A. Garavaglia, G. Giusto, R. Bottini, D. Brazzelli, *Microelectron. Eng.*, **72**, 5 (2004).
12. N. Raghavan, K. L. Pey, X. Wu, W. H. Liu, X. Li, M. Bosman, and T. Kauerauf, *IEEE Electron Device Lett.*, **32**, 252 (2011).
13. S. Lee, W. G. Kim, S. W. Rhee, and K. Yong, *J. Electrochem. Soc.*, **155**, H92 (2008).
14. M. Terai, Y. Sakotsubo, S. Kotsuji, and H. Hada, *IEEE Electron Device Lett.*, **31**, 204 (2010).
15. L. Goux, P. Czarnecki, Y. Y. Chen, L. Pantisano, X. P. Wang, R. Degraeve, B. Govoreanu, M. Jurczak, D. J. Wouters, L. Altimime, *Appl. Phys. Lett.*, **97**, 243509 (2010).
16. L. Wang, K.-J. Jin, G. Chen, C. Wang, H.-Z. Guo, H.-B. Lu, and G.-Z. Yang, *Appl. Phys. Lett.* **102**, 252907 (2013).
17. J. Park, S. Lee, J. Lee, K. Yong, *Adv. Mater.*, 25, 6423 (2013).
18. Y. M. Cui, W. Liu, R. M. Wang, *Phys. Chem. Chem. Phys.*, **15**, 6804 (2013).
19. B. Sun and C. M. Li, *Phys. Chem. Chem. Phys.*, **17**, 6718 (2015).
20. T. Kawashima, K. S. Yew, Y. Zhou, D. S. Ang, M. K. Milan, and H. Z. Zhang, *IEEE Electron Device Lett.*, in press.
21. Y. Zhou, K. S. Yew, D. S. Ang, T. Kawashima, M. K. Milan, H. Z. Zhang, *Appl. Phys. Lett.*, in press.
22. M. Ceschia, A. Paccagnella, S. Sandrin, G. Ghidini, J. Wyss, M. Lavale, O. Flament, *IEEE Trans. Nucl. Sci.*, **47**, 566 (2000).
23. A. Y. Kang, P. M. Lenahan, J. F. Conley, *IEEE Trans. Nucl. Sci.*, **49**, 2636 (2002).
24. B. Cappella and G. Dietler, *Surf. Sci. Report*, **34**, 1 (1999).
25. F. Monsieur, E. Vincent, D. Roy, S. Bruyere, J. C. Vildeuil, G. Pananakakis, and G. Ghibaudo, in Proc. Int. Reliab. Phys. Symp. 2002, 45.
26. M. Ziegler, R. Soni, T. Patelczyk, M. Ignatov, T. Bartsch, P. Meuffels, and H. Kohlstedt, *Adv. Mat.* **22**, 2744 (2012).
27. G. Bersuker, and D. C. Gilmer, *Advances in Nonvolatile Memory and Storage Technology*, Vol. 64, p. 288, Woodhead Publishing (2014**)**.
28. P. Calka, E. Martinez, V. Delaye, D. Lafond, G. Audoit, D. Mariolle, N. Chevalier, H. Grampeix, C. Cagli, V. Jousseaume, and C. Guedj, *Nanotechnol.*, 24, 085706 (2013).
29. S. Privitera, G. Bersuker, B. Butcher, A. Kalantarian, S. Lombardo, C. Bongiorno, R. Geer, D. C. Gilmer, and P. D. Kirsch, *Microelectron. Eng.*, **109**, 75 (2013).
30. B. Butcher, G. Bersuker, L. Vandelli, A. Padovani, L. Larcher, A. Kalantarian, R. Geer, and D. C. Gilmer, in *Proc. Int. Memory Workshop* 2013, 52.
31. K. P. McKenna and A. L. Shluger, *Microelectron. Eng.*, 86, 1751 (2009).
32. D. M. Duffy, S. L. Daraszewicz, and J. Mulroue, *Nucl. Instru. Method. Phys. Res. B*, **277**, 21 (2012).